

Cosmogenic ^{10}Be surface exposure dating of 'Little Ice Age' glacial events in the Mount Jaggang area, central Tibet

The Holocene
1–10
© The Author(s) 2017
Reprints and permissions:
sagepub.co.uk/journalsPermissions.nav
DOI: 10.1177/0959683617693895
journals.sagepub.com/home/hol


Guocheng Dong,^{1,2} Weijian Zhou,^{1,2,3} Chaolu Yi,^{4,5} Li Zhang,^{1,2}
Ming Li,^{1,2} Yunchong Fu^{1,2} and Qian Zhang⁴

Abstract

The timing and extent of 'Little Ice Age' (LIA) glacial advances on the Tibetan Plateau (TP) are critical for understanding climate during the past millennium. However, the lack of LIA chronologies in central Tibet makes it difficult to fully understand the nature of LIA throughout the TP. In this study, two presumed LIA moraines in the east of Mount Jaggang, Xainza range, the central TP, were examined and dated using ^{10}Be surface exposure dating. Eight boulders from the two moraines yielded apparent ^{10}Be exposure-ages ranging from 41 ± 31 to 529 ± 130 years. These ^{10}Be exposure-ages indicate that glaciers advanced at least once in the Mount Jaggang area during the LIA. A relatively extensive glacial advance occurred around 267 ± 36 years, a relatively humid period as indicated by proxy data from lake sediments in the central TP. A glacial standstill might have occurred around 151 ± 36 years. The two LIA glacial events are comparable with those across the TP. However, much more efforts should be made on dating of LIA moraines in the Mount Jaggang area to elucidate the relationships between glacial advances and climate changes during the LIA.

Keywords

^{10}Be surface exposure dating, central Tibet, glacial advances, 'Little Ice Age', Mount Jaggang, Xainza range

Received 11 August 2016; revised manuscript accepted 13 January 2017

Introduction

The term 'Little Ice Age' (LIA), originally coined by Matthes (1939), represents a well-recognized cold period in the past millennium (Mann et al., 2009), which has been extensively recorded in historical archives and proxy data from around the world, such as ice cores, tree rings, and sediments (e.g. Jones and Mann, 2004; Jones et al., 1998; Luckman, 2000; Pfister et al., 1998; Yao et al., 1997; Zhu et al., 2013). This period is conventionally defined as 16th–19th centuries in Europe (Grove, 1988; Pfister et al., 1998) and is expanded to 14th–19th centuries elsewhere in the world (Mann, 2002; Mann et al., 2009). In spite of a global cold event, the timing and intensity of LIA vary highly between regions (Bradley and Jones, 1993; Chenet et al., 2010; Jones et al., 1998, 1999; Mann et al., 1999). This draws our attentions to the timing and pattern of LIA glacial activities in glacierized mountains, such as those on the Tibetan Plateau (TP) and its surroundings (e.g. Xu and Yi, 2014 and references therein), and their relationships with climate change.

The TP contains the largest number of glaciers outside the polar regions (Haeberli et al., 1989) and links the regional and global climates through initiating the Asian monsoon and separating the Northern Hemisphere westerly into two branches (An et al., 2001; Benn and Owen, 1998; Monlar and England, 1990; Prell and Kutzbach, 1992; Raymo and Ruddiman, 1992). Glaciers therein react sensitively to climate change (Yao et al., 2012a, 2012b). Understanding the timing and nature of LIA glacial fluctuations on the TP could thus provide insights into clarifying climate changes over the past millennium in regional and global scales.

Since the past decades, a large number of studies have involved the LIA glacial fluctuations in the TP and its neighboring mountains (e.g. Chen et al., 2015; Li and Li, 2014; Li et al., 2014, 2016; Loibl et al., 2014; Owen et al., 2010; Seong et al., 2007, 2009; Su and Shi, 2002; Wang, 1991; Zhang, 1988). The LIA glacial fluctuations on the TP were argued to mainly respond to changes in temperature (Xu and Yi, 2014). However, as emphasized by Xu and Yi (2014), these studies mainly concentrate on the marginal mountains of TP. No study of mountains (such as Mount Jaggang) on the central Tibet has yet dated the LIA moraines, despite examination of the presumed LIA moraines (Lehmkuhl et al., 2002). The lack of LIA chronologies on the central TP impedes a

¹State Key Laboratory of Loess and Quaternary Geology, Institute of Earth Environment, Chinese Academy of Sciences, China

²Xi'an AMS Center, China

³Beijing Normal University, China

⁴Key Laboratory of Tibetan Environment Changes and Land Surface Process, Chinese Academy of Sciences, China

⁵Excellence Center for Tibetan Plateau Research, Chinese Academy of Sciences, China

Corresponding author:

Guocheng Dong, State Key Laboratory of Loess and Quaternary Geology, Institute of Earth Environment, Chinese Academy of Sciences, Xi'an 710061, China.

Email: donggc@ieecas.cn

comparison of LIA glacial advances across the TP and a full understanding of correlations between LIA glacial fluctuations and climate changes on the whole TP. The recent improvements in cosmogenic surface exposure dating on glacial landforms (Balco, 2011) allow us to examine the timing of LIA glacial advances on the central TP.

In this study, aiming to constrain the timing and extent of LIA glacial advances on the central TP, we examined the presumed LIA moraines in the east of Mount Jaggang, the Xainza range, and dated them using ^{10}Be surface exposure dating. We then compared the LIA chronologies with proxy records to examine the relationships between glacial fluctuations and climate changes during the LIA.

Study area

Mount Jaggang (30.8°N, 88.6°E), at 6444 m a.s.l., is the highest peak of the Xainza range, which lies on the southern part of the central TP (Figure 1a), where the southwest monsoon and mid-latitude westerly dominate, in summer and winter, respectively (Dong et al., 2010). During 1981–2012, the mean annual temperature is recorded to 0.55°C in the Xainza County, ~13 km north of Mount Jaggang (Figure 1b), and the mean annual precipitation is recorded to 316 mm, with 90% falling in June–September (Li et al., 2015).

Our study area is located on the east slope of Mount Jaggang, where one east-facing glacial catchment comprises two glacial valleys (Figure 2a). The main valley originates from Mount Jaggang and stretches ~3 km to the mountain front at an altitude of 5368 m a.s.l.; the hanging valley, whose head lies ~900 m east of Mount Jaggang, extends ~1.7 km northeastward and merges with the main valley at an altitude of ~5390 m a.s.l. (Figure 2a). Currently, glaciers can be identified in both the two valleys: glacier deriving from Mount Jaggang descends to an altitude of 5505 m a.s.l. in the main valley; and glacier in the hanging valley ends at an altitude of 5605 m a.s.l. (Figure 2a).

In addition to modern glaciers, two sets of moraines can be distinguished in the main valley (Figures 2 and 3). A set of latero-frontal moraine (numbered M1 in this study) rises ~30 m above the glacier front, and extends ~900 m along the valley wall to an altitude of ~5360 m a.s.l. (Figure 2a). This fresh-looking moraine is characterized by a sharp-crested ridge (Figure 3a–c), which is composed of fine and coarse sands, cobbles, and granitic and granite-gneissic boulders. Besides this till, sparse vegetation can be identified on moraine M1. A set of younger-looking marginal moraine (referred to as moraine M2 hereafter) is distributed within 500 m beyond the glacier terminus, and is ~1–2 m higher than the valley floor. Characteristically, moraine M2 presents limited evidences of weathering, soil development, and vegetation cover (Figure 3d–f). Yet, this moraine is rich in granitic sub-angular boulders, which feature fresh surfaces and have diameters up to 3 m (Figure 3f). The two moraines, M1 and M2, can be traced upstream to two sets of trimlines (Figures 2 and 3). Besides the trimlines, other glacially sculptured landforms, including glacially polished surface and ice-sculptured bedrocks, can also be recognized in the glacial catchment (Figures 2 and 3).

Methods

Sampling

The LIA moraines commonly lie downstream within a few hundred meters from a glacier terminus and feature fresh-looking, sharp-crested, and boulder-compact ridges (Matthes, 1939). Two or three moraines have been proposed to be formed during the LIA throughout the TP and its surroundings (Xu and Yi, 2014). Prior to the fieldwork, the two LIA moraines were initially identified and delineated in Google Earth (Figure 2b). The two moraines

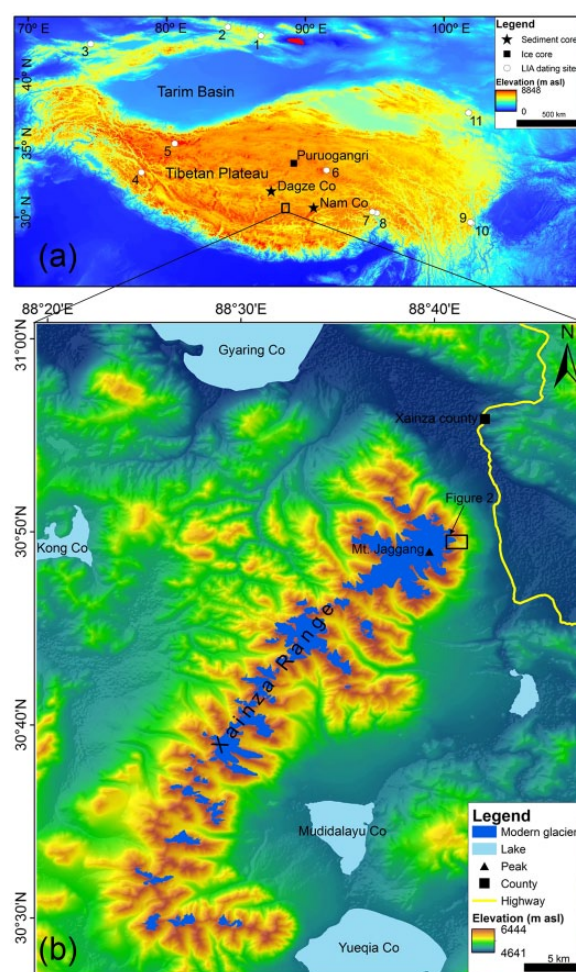


Figure 1. Map showing the location of the study area. (a) Overview of the location of the study area. White circles are locations of the LIA glacial advances discussed in this study: (1) No. 1 glacier (Chen, 1989), (2) Haxilegen Pass (Li et al., 2016), (3) Ala Archa (Koppes et al., 2008), (4) Ayizhisu (Ono et al., 1997), (5) Puga (Hedrick et al., 2011), (6) Poge (Li et al., 1986), (7) Zepu (Jiao et al., 2005), (8) Ruoguo (Li et al., 1986), (9) Hailuogou (Zheng and Ma, 1994), (10) Yanzigou (Smiraglia, 1997), (11) Shuiguanhe (Wang, 1991). Proxy date sites are shown by black rectangle and stars: an ice core from Puruogangri ice field (Thompson et al., 2006), and lake sediment core from Dagze Co (Li et al., 2015) and Nam Co lake (Zhu et al., 2008). (b) The specific location of Mount Jaggang at the Xainza range.

were then examined during the fieldwork in 2014 to define moraine ridges being suitable for ^{10}Be surface exposure dating.

We preferred quartz-rich granitic glacial boulders, featuring rock varnish on their surfaces, for ^{10}Be surface exposure dating. Four glacial boulders were sampled from moraine M1 and M2, respectively. Rock chips of <5 cm thickness were collected from the top surface of boulders using hammer and chisel. Longitude, latitude, and elevation of all samples were recorded using a handheld GPS (global positioning system) instrument (Table 1). The lithology and size were also recorded in the field, and are presented in Table 1. Topographic shielding was calculated by using a Python tool from Li (2013) and the 30-m ASTER DEM with designated 5° intervals in both azimuth and elevation angles.

Laboratory method

Sample preparations and ^{10}Be measurements were all performed in Xi'an Accelerator Mass Spectrometry Center (Xi'an-AMS center), Institute of Earth Environment, Chinese Academy of Sciences.

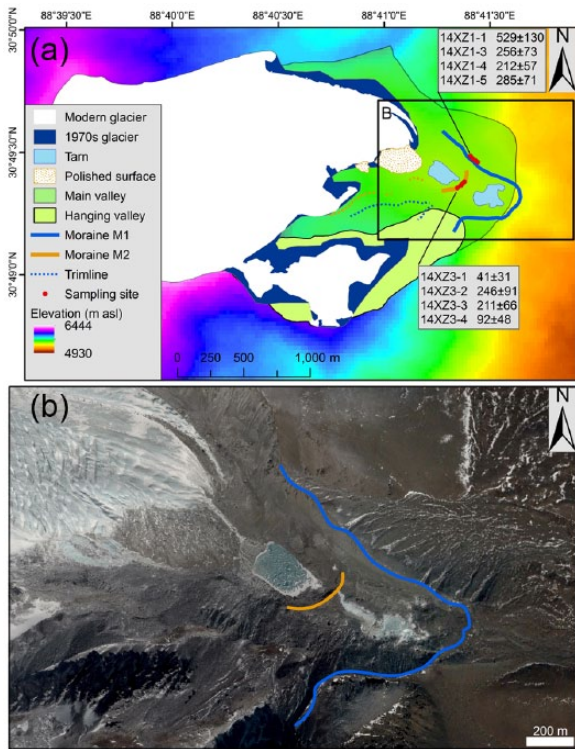


Figure 2. Geomorphic setting of the east of Mount Jaggang. (a) Overview of the east of Mount Jaggang. Modern glaciers are in white, and the mid-1970s glaciers are derived from Landsat MSS image (<http://www.gscloud.cn/>). ^{10}Be exposure-ages are given in unit of years in the gray boxes. (b) Oblique Google Earth image showing the presumed LIA moraines. The colored lines identify the two LIA moraines that are illustrated in Figure 2a following the same color scheme.

Quartz isolation, dissolution, chromatography, isolation of Be, and preparation of BeO were undertaken following the revised procedure of Kohl and Nishiizumi (1992), as described in detail by Dong et al. (2014). The $^{10}\text{Be}/^9\text{Be}$ ratios were measured based on the revised ICN standard (07KNSTD; Nishiizumi et al., 2007). The measured $^{10}\text{Be}/^9\text{Be}$ ratios were corrected with two chemical procedural blanks (4.96×10^{-15} and 4.32×10^{-15}) and converted to ^{10}Be concentrations for exposure-age calculation (Table 1). Quartz weights, ^9Be carrier masses, measured $^{10}\text{Be}/^9\text{Be}$ ratios, and procedural blanks are shown in the Supplementary Material, available online.

Exposure-age calculation and moraine age determination

Cosmogenic ^{10}Be exposure-ages were calculated using the CRO-NUS online calculator version 2.3 (<http://hess.ess.washington.edu/math/>; Balco et al., 2008). We focused on exposure-ages derived from Lal (1991)/Stone (2000) time-independent scaling scheme. Rock densities were assigned to be 2.7 g/cm^3 . No corrections were carried out for erosion or snow cover in this study.

In ideal situations, exposure-ages of boulders should represent the moraine depositional age, but geomorphic process commonly results in scattered exposure-ages on a moraine (Heyman et al., 2011). Different strategies have been used to interpret age-scatters and to identify outliers (e.g. Balco, 2011 and references therein). In this study, the reduced chi-square (χ_R^2) test was used to determine whether the age-scatter could be solely explained by measurement uncertainties (Balco, 2011; Balco and Schaefer, 2006; Chen et al., 2015; Heyman, 2014; Li et al., 2014, 2016; Rood et al., 2011), and probability density functions of all ^{10}Be exposure-ages were plotted for each moraine using their internal uncertainties to help identify clustered ages and potential outliers (Chen et al., 2015; Dong et al., 2014; Li et al., 2014; Wang et al., 2013). If the χ_R^2 value is

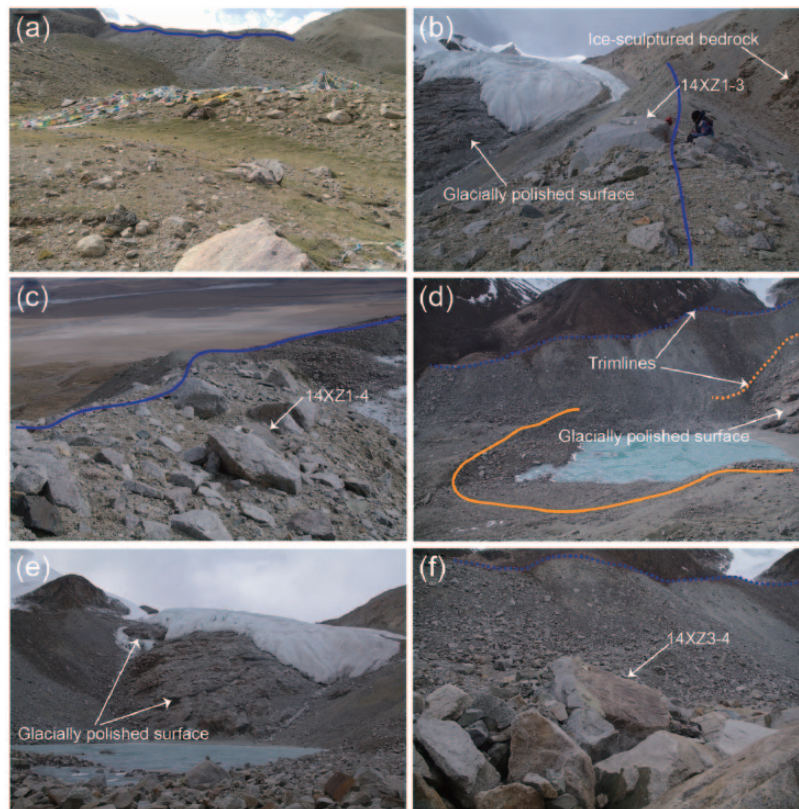


Figure 3. Selected photos of glacial landforms in the east of Mount Jaggang. (a) View of moraine M1 (blue line) at a pre-LIA moraine. (b) View up-valley on moraine M1. The sampled boulder (14XZ1-3), polished surface, and ice sculptured bedrock are illustrated by the white arrows. (c) View downstream on moraine M1. The sample 14XZ1-4 is shown in the medium shot. (d) An overlooking of moraine M2 (brown line in the foreground) and trimlines (blue and brown dashed lines in the background). (e) View toward west on moraine M2. (f) View toward south on moraine M2. Boulder in the medium shot is 14XZ3-4. In the perspective, trimline is illustrated by the blue dashed line.

Table 1. Geographical coordinates, ^{10}Be concentrations, and other parameters for boulder samples.

Moraine	Sample ID	Latitude ($^{\circ}\text{N}$)	Longitude ($^{\circ}\text{E}$)	Elevation (m a.s.l.)	Rock type	Boulder/knob size (L/W/H) (cm)	Sample thickness (cm)	Shielding factor	^{10}Be concentration (atoms/g)
M1	14XZ1-1	30.8243	88.68991	5453	Granite	120/80/60	2.108	0.96768	$44,826 \pm 10,370$
	14XZ1-3	30.82429	88.69001	5464	Granite	180/140/90	3.737	0.96768	$21,508 \pm 5863$
	14XZ1-4	30.82388	88.69048	5459	Granitic gneiss	80/65/45	4.193	0.96768	$17,650 \pm 4512$
	14XZ1-5	30.82395	88.69046	5461	Granite	200/180/90	4.767	0.96768	$23,717 \pm 5532$
M2	14XZ3-1	30.82247	88.68933	5397	Granite	185/95/88	4.553	0.98201	3347 ± 2514
	14XZ3-2	30.82236	88.68917	5383	Granite	75/59/53	1.185	0.98201	$20,658 \pm 7443$
	14XZ3-3	30.82243	88.68924	5385	Granite	97/61/60	1.161	0.98201	$17,794 \pm 5374$
	14XZ3-4	30.82234	88.68904	5384	Granite	300/250/120	2.054	0.98201	7705 ± 3936

Table 2. ^{10}Be exposure-ages calculated using two scaling schemes in the CRONUS online calculator (version 2.3).

Moraine	Sample ID	Exposure-ages (years)		
		Time-independent Lal (1991)/Stone (2000)	Time-dependent Lal (1991)/Stone (2000)	Internal uncertainty
M1	14XZ1-1	529 ± 130	605 ± 151	122
	14XZ1-3	256 ± 73	299 ± 86	70
	14XZ1-4	211 ± 57	247 ± 67	57
	14XZ1-5	285 ± 71	333 ± 84	71
M2	14XZ3-1	41 ± 31	47 ± 36	31
	14XZ3-2	246 ± 91	286 ± 107	88
	14XZ3-3	211 ± 66	246 ± 78	64
	14XZ3-4	92 ± 48	108 ± 56	47

not statistically significant ($p > 0.05$), the scatter in the dataset can be explained solely by measurement uncertainties (Rood et al., 2011), and the weighted mean was used to constrain the moraine age. Otherwise, the visual outliers were removed to refine the χ_R^2 value and re-test its significance. If the re-tested χ_R^2 value is not statistically significant ($p > 0.05$), the weighted mean was used for the age of moraine (Chen et al., 2015; Li et al., 2016).

Determination of variations in glacier length and ELA

To quantify variations in glacial extent during the LIA in the east of Mount Jaggang, we evaluated changes in glacier length and equilibrium-line-altitude (ELA). The changes in glacier length were determined using the distance from the LIA moraines to the current glacier snout. The ELA depressions were estimated based on ELAs calculated using the accumulation-area ratio (AAR) and area-altitude balance ratio (AABR) methods, which have been widely used to estimate the former ELAs throughout the TP and its surroundings (e.g. Benn and Lehmkuhl, 2000 and references therein). Details of the two methods have been reviewed by many researchers (e.g. Benn et al., 2005 and references therein). In this study, we used an AAR value of 0.6 ± 0.05 as commonly suggested for the mid-latitude glaciers (Benn and Lehmkuhl, 2000; Benn et al., 2005) and the globally average AABR value of 1.75 ± 0.71 (Rea, 2009). The calculation of LIA ELAs was carried out using the toolboxes, developed by Pellitero et al. (2015, 2016), in the ArcGIS environment. Also, the modern ELA was calculated using the toolbox in the ArcGIS environment with the same AAR and AABR ratios as for the LIA ELAs.

Results

Exposure-ages and interpretations

Eight glacial boulders from the east of Mount Jaggang have apparent exposure-ages ranging from 41 ± 31 years to 529 ± 130 years (Table 2; Figures 2 and 4).

The four glacial boulders sampled from moraine M1 dated to 211 ± 57 , 256 ± 73 , 285 ± 71 , and 529 ± 130 years, respectively. The reduced chi-square statistic on this age group has a value of 2.56 ($p > 0.05$) (Figure 4a), which implies that the weighted mean of the four ages (267 ± 36) can be used to represent the moraine depositional age. We, therefore, assigned 267 ± 36 years as the depositional age of moraine M1.

The younger-looking moraine (M2) produced four scattered apparent exposure-ages: 41 ± 31 years, 92 ± 48 years, 211 ± 66 years, and 246 ± 91 years, which are all within the span of LIA period except the youngest one. If the youngest exposure-age is removed, the χ_R^2 value is reduced from 5.14 ($p < 0.05$) to 2.23 ($p > 0.05$), enabling the weighted mean of the remaining three exposure-ages, 151 ± 36 years, to represent the formation age of moraine M2.

Variations in glacier length, area, and ELA

The changes in glacier length marked by moraine M1 and M2 are presented in Table 3. The ELAs estimated using AAR and AABR methods are presented in Figure 5, and the ELA depressions are calculated and listed in Table 3.

Discussion

Timing of LIA glacial events in Mount Jaggang

Moraine M1 yields relatively robust age cluster that can be used to constrain the moraine depositional age. The weighted mean of the four exposure-ages from this moraine constrains the timing of the LIA glacial advance to 267 ± 36 years.

Inversely, however, the younger-looking moraine (M2) generates widely spread exposure-ages. One boulder produces an apparently young exposure-age of 41 ± 31 years. If this exposure-age represents the moraine depositional age, moraine M2 should be deposited during the 1970s. To examine the glacial fluctuations during the 1970s, we checked the Landsat MSS image produced in the mid-1970s (<http://www.csdb.cn/>). The image

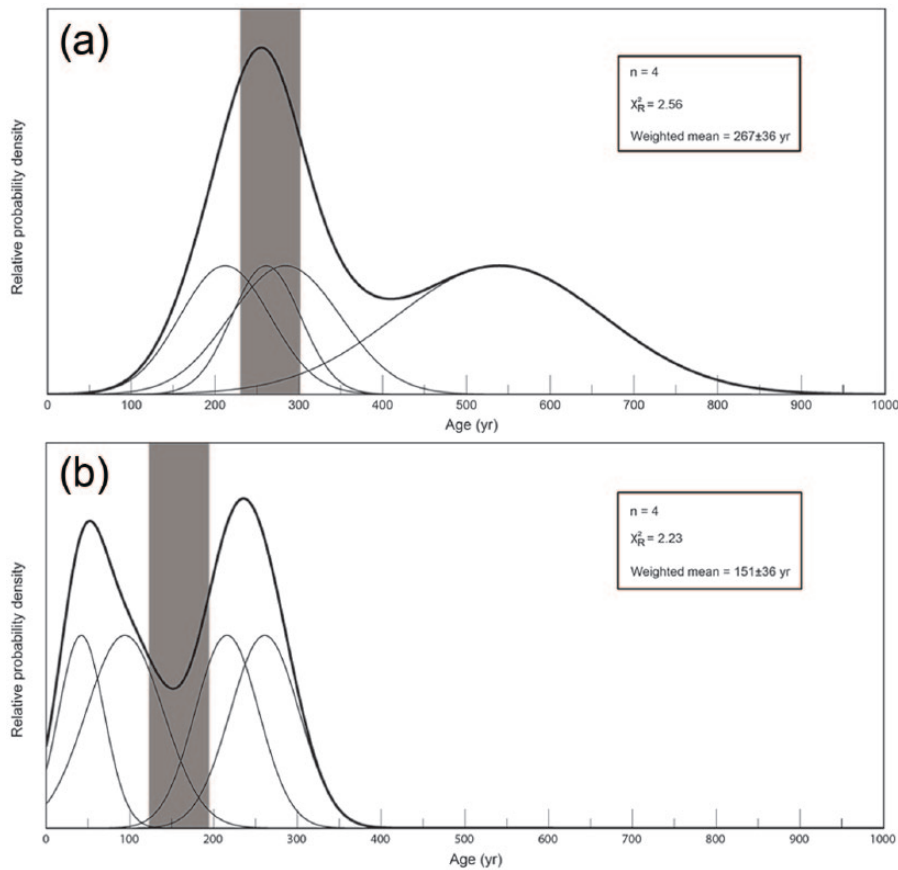


Figure 4. Probability density plots of ^{10}Be exposure-ages for moraine (a) M1 and (b) M2. Individual age is plotted as a probability density function (PDF) of a normal distribution using the exposure-age and internal uncertainty. The individual PDF is normalized to 1 and is illustrated by black thin curves. The cumulative PDF is created by summing individual PDF and shown by the black thick curve. The values of reduced chi-square statistic ($p > 0.05$) are listed on the plot. The weighted mean and weighted uncertainty (one sigma) are also listed and depicted by the gray column on the plot, with the weighted uncertainty (one sigma).

Table 3. Glacier area, retreat distance, and estimated change in ELA (ΔELA) from LIA glaciers to current glaciers in the east of Mount Jaggang area.

LIA event	Area (km^2)	Distance (m)	ΔELA (m)	
			AAR	AABR
Glacial advance	0.82	900–1000	124–164	84–164
Glacial standstill	0.3	500	29–69	49–69

ELA: equilibrium-line-altitude; LIA: ‘Little Ice Age’; AAR: accumulation-area ratio; AABR: area-altitude balance ratio.

indicates that glacier extent was limited in the mid-1970s, compared with that marked by moraine M2 (Figure 2). Thus, we conclude that this young boulder has experienced incomplete exposure, potentially caused by toppling or shielding from other boulders. The weighted mean of the remaining three exposure-ages constrain the formation age of moraine M2 to 151 ± 36 years. Note, however, that moraine M2 rises merely ~ 1 – 2 m over the valley floor. Such a moraine commonly implies a recessional moraine formed during temporary halt in a glacier retreat (Benn and Evans, 2010). Moraine M2 thus likely marks a glacial standstill around 151 ± 36 years.

While the timing of the two LIA events, so far, has been constrained by assuming that age-scatters can be explained solely by measurement uncertainties, the possibility of effects from geomorphic processes, especially prior exposure, cannot be fully excluded at present. This is due to that the small and thin glaciers, such as those in the east of Mount Jaggang, are probably lack of

enough erosional power to produce fresh boulders with zero initial nuclide concentration (Li et al., 2016), especially during a short glacial standstill.

Overall, cosmogenic ^{10}Be exposure-ages suggest that a relatively extensive glacial advance occurred at 267 ± 36 years in the Mount Jaggang area during the LIA and that a glacial standstill occurred around 151 ± 36 years. The two dated LIA glacial events are comparable with those revealed by radiocarbon (Jiao et al., 2005; Ono et al., 1997; Smiraglia, 1997; Zheng and Ma, 1994), lichenometry (Chen, 1989; Li et al., 1986; Wang, 1991), and ^{10}Be surface exposure datings (Hedrick et al., 2011; Koppes et al., 2008; Li et al., 2016) on the TP and its surroundings.

To compare LIA chronologies between regions across the TP, the available published ^{14}C ages were calibrated using the software CALIB 7.1 (Reimer et al., 2013), and ^{10}Be exposure-ages were recalculated using the method described in ‘Laboratory method’ section. These ages were then given in calendar year (Table 4). When converting these recalculated ages to calendar year, year of sampling is based on information in the sources if available, and is otherwise assumed to be two years before publication.

Several studies have suggested that the LIA maximum extent occurred roughly between AD 1700 and AD 1800. For example, Hedrick et al. (2011) obtained six ^{10}Be exposure-ages ranging from 207 to 1340 years on a moraine in the Puga Valley, Zaskar range, western Himalaya (Table 4). After removing three outliers, Xu and Yi (2014) considered that this moraine was deposited between AD 1719 and AD 1802. Li et al. (1986) defined three LIA moraines in the front of Poga glacier, Tanggula Shan, the central TP using lichenometric dating. The lichenometric dating results

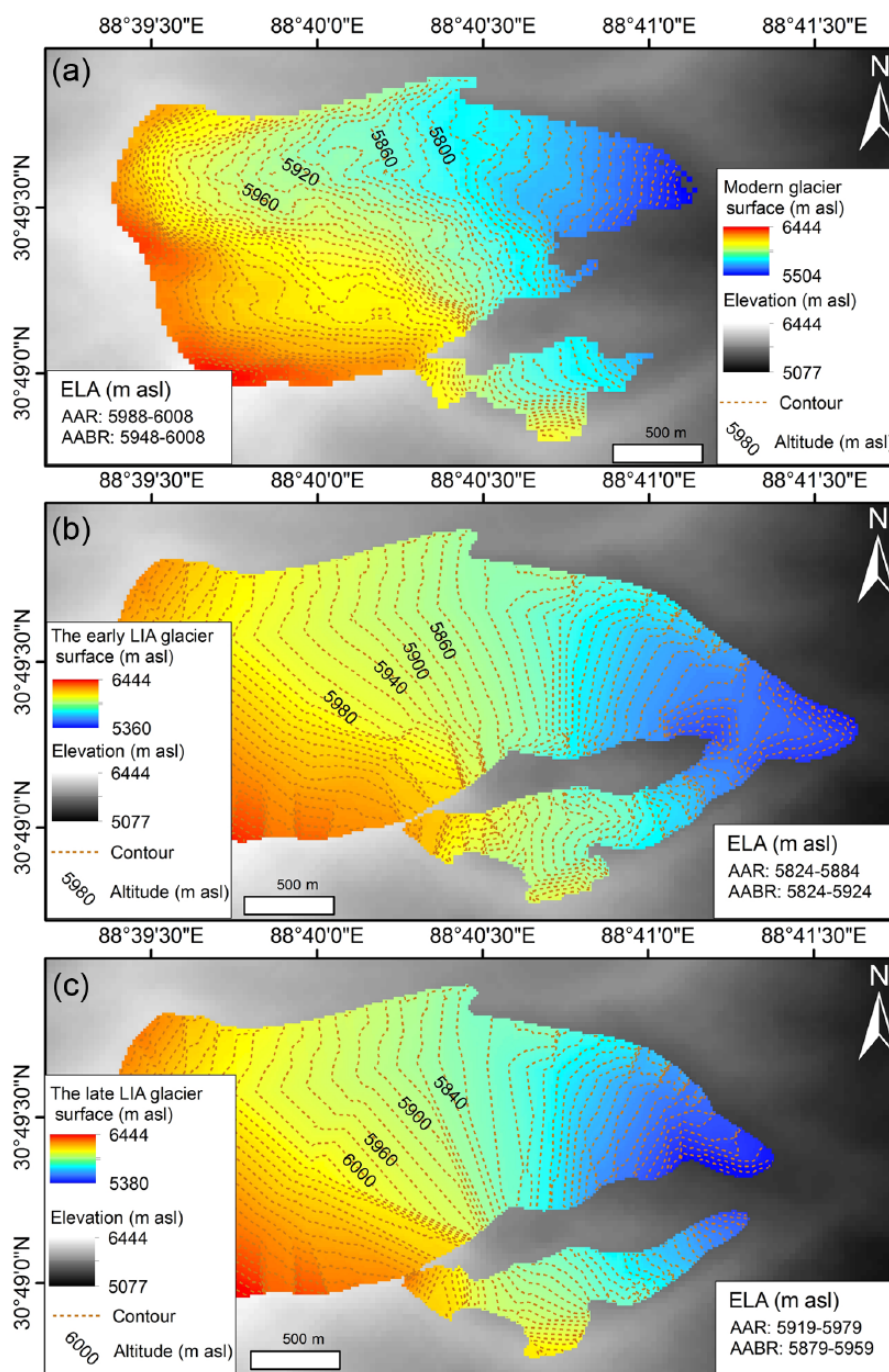


Figure 5. The (a) modern and (b and c) reconstructed LIA glacier surfaces used to estimate ELA depressions during the LIA.

indicate that the outermost moraine was formed at AD 1809 (Table 4). Also, the LIA glacial advances spanning AD 1700–1800 are evidenced in other regions of the TP, although not the maximum, such as the Pamir (Ono et al., 1997), the Nyainqentanglha Shan (Jiao et al., 2005; Li et al., 1986) and Hengduan Shan (Smiraglia, 1997; Zheng and Ma, 1994), the southeastern TP, Qilianshan (Wang, 1991), the northeastern TP, and Tian Shan (Chen, 1989; Koppes et al., 2008; Li et al., 2016) (Table 4). Additionally, among these regions, the glacial advance after AD 1800 can be distinguished in the Tanggula Shan (Li et al., 1986), Nyainqentanglha Shan (Li et al., 1986), Qilian Shan (Wang, 1991), and Tian Shan (Chen, 1989).

The extent of LIA glacial events in Mount Jaggang

The locations of moraines and associated trimlines imply that moraine M1 was deposited by the compound glacier from the main valley and the hanging valley and that moraine M2 was

formed by the glacier in the main valley. In view of the moraine deposition, moraine M1 indicates that glaciers have shrunk ~900–100 m in length and ~0.82 km² in area since AD 1747 ± 36 in the east of Mount Jaggang (Figure 2b). Moraine M2 illustrates that glacier in the main valley has retreated ~500 m and shrunk ~0.3 km² since AD 1863 ± 36. However, it is hard to define the changes in glacier length after AD 1863 ± 36 in the hanging valley because no moraine has been identified in this valley. The estimated LIA and modern ELAs (Figure 5) indicate that ELAs in the east of Mount Jaggang have increased ~84–164 m for the past 267 ± 36 years and increased ~29–69 m since the glacial standstill around AD 1863 ± 36.

Climatic implication on LIA glacial advances of Mount Jaggang

The last millennial climates on the central TP have been reconstructed using proxy data from ice core and lake sediment

Table 4. LIA glacial chronologies that are comparable with those in the east of Mount Jaggang in the other regions of TP.

Site	Glacier/valley	Location	Elevation (m a.s.l.)	Dating material/method	Sample ID	Published age	Recalculated age	Recalculated age (Calendar year)	Source
Himalayas	Puga	33.23/78.17	5266	Boulder/ ¹⁰ Be	India-45	460 ± 50 years	506 ± 55 years	AD 1503	Hedrick et al. (2011)
		33.23/78.17	5263		India-46	190 ± 30 years	207 ± 30 years	AD 1802	
		33.23/78.17	5257		India-47	1220 ± 120 years	1340 ± 126 years	AD 669	
		33.23/78.17	5267		India-48	1050 ± 100 years	1152 ± 112 years	AD 857	
		33.23/78.17	5260		India-49	250 ± 40 years	276 ± 43 years	AD 1733	
Pamir Plateau	Ayizhisu	33.23/78.17	5265		India-50	260 ± 40 years	290 ± 46 years	AD 1719	
		—	—	Buried wood/ ¹⁴ C	AYZS1 ^a	110 ± 50 yr BP	125 ± 43 yr BP	AD 1825 ± 43	Ono et al. (1997)
Nyainqentangha Shan	Zepu	—	—	Buried wood/ ¹⁴ C	AYZS2 ^a	200 ± 50 yr BP	183 ± 37 yr BP	AD 1767 ± 37	
		30.30/95.15	2995	Buried wood/ ¹⁴ C	I-16138	190 ± 80 yr BP	186 ± 45 yr BP	AD 1764 ± 45	Jiao et al. (2005)
Tanggula Shan	Ruoguo	—	—	Lichens on glacial boulder	RG ^a	197 ± 80 yr BP	191 ± 45 yr BP	AD 1759 ± 45	Li et al. (1986)
		—	—	Lichens on glacial boulder	PG1 ^a	AD 1822			Li et al. (1986)
		—	—	Lichens on glacial boulder	PG2 ^a	AD 1902			
Qilian Shan	Shuiguanhe	—	—	Lichens on glacial boulder	PG3 ^a	AD 1857			
		—	—	Lichens on glacial boulder	PG4 ^a	AD 1888			
		—	—	Lichens on glacial boulders	SGH1 ^a	AD 1809			Wang (1991)
		—	—	Lichens on glacial boulders	SGH2 ^a	AD 1762 ± 20			
Tianshan	Ala Archa	—	—	Lichens on glacial boulders	KTS98-CS-101	AD 1857 ± 20			Koppes et al. (2008)
		42.52/74.51	3246	Boulder/ ¹⁰ Be	NG1 ^a	250 ± 100 years	268 ± 71 years	AD 1738	Chen (1989)
Haxilegen Pass	No. 1 Glacier	—	—	Lichens on glacial boulders	NG2 ^a	AD 1777 ± 20			
		43.7385/84.4024	3484	Lichens on glacial boulders	HDB-12-06	AD 1871 ± 20			Li et al. (2016)
		43.7385/84.4025	3485	Boulder/ ¹⁰ Be	HDB-12-07	222 ± 21 years	194 ± 23 years	AD 1818	
		43.7384/84.4028	3481	Boulder/ ¹⁰ Be	HDB-12-08	286 ± 31 years	250 ± 32 years	AD 1762	
		43.7380/84.4033	3483	Boulder/ ¹⁰ Be	HDB-12-09	825 ± 82 years	746 ± 91 years	AD 1266	
		43.7380/84.4034	3485	Boulder/ ¹⁰ Be	HDB-12-10	587 ± 49 years	519 ± 57 years	AD 1493	
		43.7372/84.4073	3411	Boulder/ ¹⁰ Be	HDB-12-16	232 ± 25 years	224 ± 29 years	AD 1788	
		43.7373/84.4069	3418	Boulder/ ¹⁰ Be	HDB-12-17	284 ± 63 years	248 ± 57 years	AD 1764	
		43.7372/84.4068	3417	Boulder/ ¹⁰ Be	HDB-12-18	135 ± 22 years	118 ± 21 years	AD 1894	
		43.7372/84.4063	3420	Boulder/ ¹⁰ Be	HDB-12-19	266 ± 42 years	232 ± 40 years	AD 1780	
Hengduan Shan	Hailuoguo	43.7370/84.4062	3424	Boulder/ ¹⁰ Be	HDB-12-20	331 ± 61 years	289 ± 57 years	AD 1723	
		—	—	Buried wood/ ¹⁴ C	LB-91014	238 ± 38 years	208 ± 36 years	AD 1804	
Yanzigou	Yanzigou	29.63/101.9	3870	Buried wood/ ¹⁴ C	GX-17452	150 ± 60 yr BP	153 ± 29 yr BP	AD 1797 ± 29	Zheng and Ma (1994)
		—	—	Buried wood/ ¹⁴ C	GX-17453	145 ± 100 yr BP	170 ± 32 yr BP	AD 1780 ± 32	Smiraglia (1997)
—	—	—	—	—	—	235 ± 110 yr BP	261 ± 39 yr BP	AD 16890 ± 39	

^aNumbered in this study.

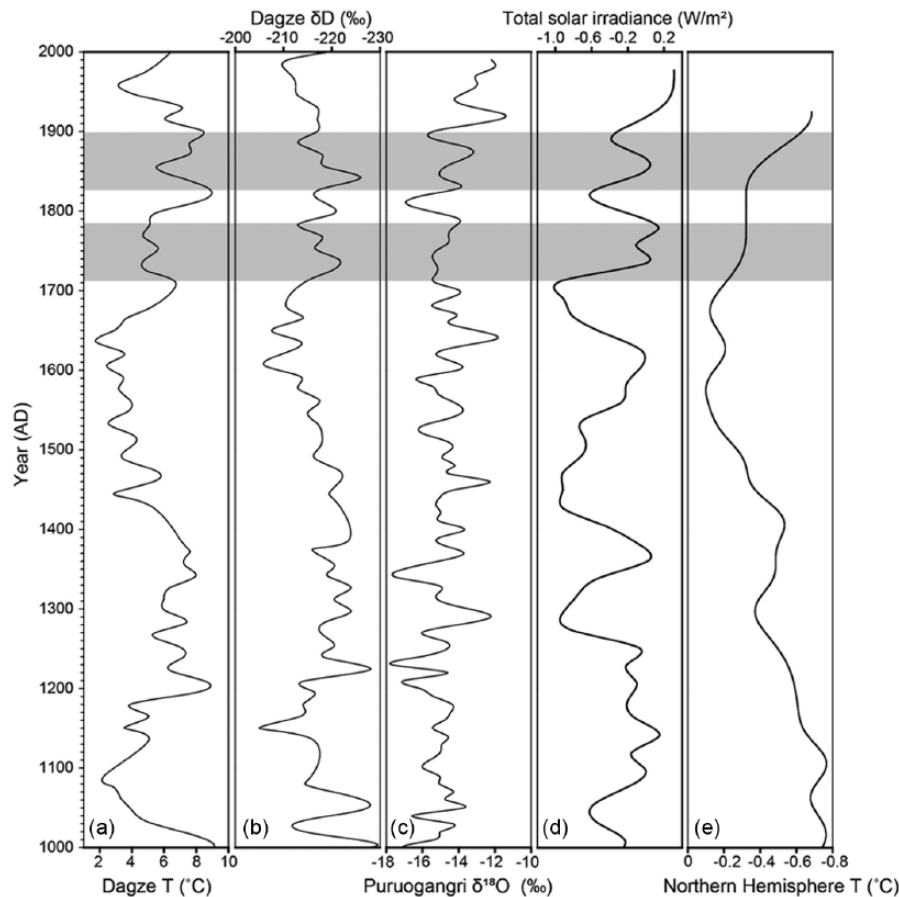


Figure 6. Comparison of the timing of LIA glacial events in the east of Mount Jaggang and selected published climate records: (a) the annual mean temperature deduced from Dagze Co (Li et al., 2015); (b) the weighted average δD value of n-alkanoic from Dagze Co, which reflect changes in precipitation (Li et al., 2015); (c) $\delta^{18}O$ records in Puruogangri ice core (Thompson et al., 2006); (d) total solar irradiance (Steinhilber et al., 2012); (e) Northern Hemisphere temperature (Moberg et al., 2005). Gray bands illustrate the timing of the LIA glacial events in the east of Mount Jaggang.

(Figures 1 and 6). Oxygen isotope records in Puruogangri ice core imply complicated climates during the past millennium (Figure 6c; Thompson et al., 2006). Despite complicated conditions revealed by oxygen isotope records from ice core, several cold and/or humid periods have been documented by lacustrine sediments from Dagze Co.

The extensive LIA glacial advance at 267 ± 36 years coincides with a relatively warm period recorded in Dagze Co, ~150 km northwest of Mount Jaggang (Figures 1, 6a and b), which is also recorded by variations in total solar radiation and Northern Hemisphere temperature (Figures 6d and e). However, variation in precipitation derived from Dagze Co reflects a relatively humid stage during ~AD 1730–1800 (Figure 6b; Li et al., 2015). The timing of this LIA glacial advance falls well into this period, implying that the precipitation of this period has contributed to this glacial advance. The post-AD 1800 is also characterized by the moderately humid conditions (Figure 6b). In addition, two or more cooling events have been revealed by proxy data from Dagze Co and Puruogangri, and variations in total solar irradiance (Figure 6a, c and d). Although the tentatively assigned timing of LIA glacial standstill broadly spans these events, it is tough to make a correlation between this LIA event and climate change.

In summary, the extensive LIA glacial advance in the Mount Jaggang area appears to respond to relatively humid climate. This implies that precipitation might play a key role in determining the glacial extent during the LIA. It should be admitted that, however, it is difficult to correlate the glacial standstill with cooling event or humid condition. Further, it is worth noting that climatic records are still rare around the Mount Jaggang area, and that more climate proxy should be reconstructed to illustrate the

correlation between glacial activities and climate changes during the LIA.

Conclusion

Eight ^{10}Be exposure-ages (41 ± 31 – 529 ± 130 years) of glacial boulders sampled from fresh moraines were used to constrain the timing and pattern of LIA glacial activities in the east of Mount Jaggang, Xainza range, the central TP. The fresh-looking outer moraine (M1) produced relatively well-clustered ages around 267 ± 36 years, implying that this moraine was formed by the LIA glacial advance around 267 years. This glacial advance appears to respond to the humid climate at that time. The inner younger-looking moraine (M2) indicates a glacial standstill around 151 ± 36 years, which is hard to be correlated with climate change at present. More efforts on LIA glacial chronologies should be conducted to better understand the spatio-temporal pattern of LIA glacial fluctuations on the central TP and its forcing mechanisms.

The two dated moraines in the east of Mount Jaggang indicate that glaciers there have shrunk ~900–1000 m in distance and ~0.82 km² in area for the past 267 ± 36 years, with an ELA increase of ~84–164 m, and that glaciers have retreated ~500 m since AD 1863 \pm 36, with area shrinkage of ~0.3 km² and ELA increase of ~29–69 m.

Acknowledgements

We are grateful to Jakob Heyman from University of Gothenburg and two anonymous reviewers for their thorough reviews that helped significantly improve this manuscript. We would like to

appreciate Juzhi Hou and Xiumei Li from Institute of Tibetan Plateau Research, Chinese Academy of Sciences for sharing climatic records from Dage Co.

Funding

This work was supported by the National Natural Science Foundation of China (Grant Nos. 40971017 and 41230523), and Strategic Priority Research Program (B) of the Chinese Academy of Sciences (XDB01020300).

References

- An Z, Kutzbach JE, Prell WL et al. (2001) Evolution of Asian monsoons and phased uplift of the Himalayan-Tibetan Plateau since Late Miocene times. *Nature* 411: 62–66.
- Balco G (2011) Contributions and unrealized potential contributions of cosmogenic-nuclide exposure dating to glacier chronology, 1990–2010. *Quaternary Science Reviews* 30: 3–27.
- Balco G and Schafer JM (2006) Cosmogenic-nuclide and varve chronologies for the deglaciation of southern New England. *Quaternary Geochronology* 1: 15–28.
- Balco G, Stone JO, Lifton NA et al. (2008) A complete and easily accessible means of calculating surface exposure ages or erosion rates from ^{10}Be and ^{26}Al measurements. *Quaternary Geochronology* 3: 174–195.
- Benn DI and Evans D (2010) *Glaciers and Glaciations*. 2nd Edition. London: Hodder Education.
- Benn DI and Lehmkuhl F (2000) Mass balance and equilibrium-line altitudes of glaciers in high-mountain environments. *Quaternary International* 65–66: 15–29.
- Benn DI and Owen LA (1998) The role of the Indian summer monsoon and the mid-latitude westerlies in Himalayan glaciation: Review and speculative discussion. *Journal of the Geological Society* 155: 353–363.
- Benn DI, Owen LA, Osmaston HA et al. (2005) Reconstruction of equilibrium-line altitudes for tropical and sub-tropical glaciers. *Quaternary International* 138–139: 8–21.
- Bradley RS and Jones PD (1993) ‘Little Ice Age’ summer temperature variations: Their nature and relevance to recent global warming trends. *The Holocene* 3: 367–376.
- Chen J (1989) Preliminary researches on lichenometric chronology of Holocene glacial fluctuations and on other topics in the headwater of Urumqi River, Tianshan Mountains. *Science in China Series B: Chemistry, Life Sciences & Earth Sciences* 32: 1487–1500.
- Chen Y, Li Y, Wang Y et al. (2015) Late quaternary glacial history of the Karlik Range, easternmost Tian Shan, derived from ^{10}Be surface exposure and optically stimulated luminescence datings. *Quaternary Science Reviews* 115: 17–27.
- Chenet M, Roussel E, Jomelli V et al. (2010) Asynchronous Little Ice Age glacial maximum extent in southeast Iceland. *Geomorphology* 114: 253–260.
- Dong G, Yi C and Caffee WM (2014) ^{10}Be dating of boulders on moraines from the last glacial period in the Nyainqentanglha mountains, Tibet. *Science China Earth Sciences* 57: 221–231.
- Dong G, Yi C and Chen L (2010) An introduction to the physical geography of the Qiangtang Plateau: A frontier for future geoscience research on the Tibetan Plateau. *Physical Geography* 31: 475–492.
- Grove JM (1988) *The Little Ice Age*. London: Methuen Publishing.
- Haeblerli W, Bösch H, Scherler K et al. (1989) *World Glacier Inventory – Status 1988*. Zurich: IAHS/UNEP/UNESCO.
- Hedrick KA, Seong Y, Owen LA et al. (2011) Towards defining the transition in style and timing of Quaternary glaciation between the monsoon-influenced Greater Himalaya and the semi-arid Transhimalaya of Northern India. *Quaternary International* 236: 21–33.
- Heyman J (2014) Paleoglaciation of the Tibetan Plateau and surrounding mountains based on exposure ages and ELA depression estimates. *Quaternary Science Reviews* 91: 30–41.
- Heyman J, Stroeven AP, Harbor JM et al. (2011) Too young or too old: Evaluating cosmogenic exposure dating based on an analysis of compiled boulder exposure ages. *Earth and Planetary Science Letters* 302: 71–80.
- Jiao K, Iwata S, Yao T et al. (2005) Variation of Zepu Glacier and environmental change in the eastern Nyainqentanglha Range since 3.2 ka BP. *Journal of Glaciology and Geocryology* 27: 74–79 (in Chinese with English Abstract).
- Jones PD and Mann ME (2004) Climate over past millennia. *Reviews of Geophysics* 42: 1–42. Available at: <http://dx.doi.org/10.1029/2003RG000143>
- Jones PD, Briffa KR, Barnett TP et al. (1998) High-resolution palaeoclimatic records for the last millennium: Interpretation, integration and comparison with General Circulation Model control-run temperatures. *The Holocene* 8: 455–471.
- Jones PD, Parker DE, Martin S et al. (1999) Surface air temperature and its changes over the past 150 years. *Reviews of Geophysics* 37: 173–199.
- Kohl CP and Nishiizumi K (1992) Chemical isolation of quartz for measurement of in-situ-produced cosmogenic nuclides. *Geochimica et Cosmochimica Acta* 56: 3583–3587.
- Koppes M, Gillespie AR, Burke RM et al. (2008) Late Quaternary glaciation in the Kyrgyz Tien Shan. *Quaternary Science Reviews* 27: 846–866.
- Lal D (1991) Cosmic ray labeling of erosion surfaces: In situ nuclide production rates and erosion models. *Earth and Planetary Science Letters* 104: 424–439.
- Lehmkuhl F, Klinge M and Lang A (2002) Late Quaternary glacier advances, lake level fluctuations and Aeolian sedimentation in Southern Tibet. *Zeitschrift für Geomorphologie Supplementary Issues* 126: 183–218.
- Li J, Zheng B, Yang X et al. (1986) *Glacier in Tibet*. Beijing, China: Science Press (in Chinese).
- Li X, Hou J, Liang J et al. (2015) Centennial-scale climate variability during the past 2000 years on the central Tibetan Plateau. *The Holocene* 25: 1–8.
- Li Y (2013) Determining topographic shielding from digital elevation models for cosmogenic nuclide analysis: A GIS approach and field validation. *Journal of Mountain Science* 10: 355–362.
- Li Y and Li Y (2014) Topographic and geometric controls on glacier changes in the central Tien Shan, China, since the Little Ice Age. *Annals of Glaciology* 55: 177–186.
- Li Y, Li Y, Harbor J et al. (2016) Cosmogenic ^{10}Be constraints on Little Ice Age glacial advances in the eastern Tian Shan, China. *Quaternary Science Reviews* 138: 105–118.
- Li Y, Liu G, Chen Y et al. (2014) Timing and extent of Quaternary glaciations in the Tianger Range, eastern Tian Shan, China, investigated using ^{10}Be surface exposure dating. *Quaternary Science Reviews* 98: 7–23.
- Loibl D, Lehmkuhl F and Griebinger J (2014) Reconstructing glacier retreat since the Little Ice Age in SE Tibet by glacier mapping and equilibrium line altitude calculation. *Geomorphology* 214: 22–39.
- Luckman BH (2000) The Little Ice Age in the Canadian Rockies. *Geomorphology* 32: 357–384.
- Mann ME (2002) *Little Ice Age*. Chichester: John Wiley & Sons, pp. 504–509.
- Mann ME, Bradley RS and Hughes MK (1999) Northern Hemisphere temperature during the past millennium: Inferences, uncertainties, and limitations. *Geophysical Research Letters* 26: 759–762.
- Mann ME, Zhang ZH, Rutherford S et al. (2009) Global signatures and dynamical origins of the Little Ice Age and medieval climate anomaly. *Science* 326: 1256–1260.

- Matthes FE (1939) Report of Committee on glaciers, April 1939. *Transactions: American Geophysical Union* 20: 518–523.
- Moberg A, Sonechkin DM, Holmgren K et al. (2005) Highly variable Northern Hemisphere temperatures reconstructed from low- and high-resolution proxy data. *Nature* 433: 613–617.
- Monlar P and England P (1990) Late Cenozoic uplift of mountain-ranges and global climate change – Chicken or egg? *Nature* 346: 29–34.
- Nishiizumi K, Imamura M, Caffee MW et al. (2007) Absolute calibration of ^{10}Be AMS standards. *Nuclear Instruments and Methods in Physics Research Section B: Beam Interactions with Materials and Atoms* 258: 403–413.
- Ono Y, Liu D and Zhao Y (1997) Paleoenvironments of Tibetan Plateau viewed from glacial fluctuations in the northern foot of the west Kunlun Mountains. *Journal of Geomorphology* 106: 184–198 (in Japanese).
- Owen LA, Yi C, Finkel RC et al. (2010) Quaternary glaciation of Gurla Mandhata (Naimon'anyi). *Quaternary Science Reviews* 29: 1817–1830.
- Pellitero R, Rea BR, Spagnolo M et al. (2015) A GIS tool for automatic calculation of glacier equilibrium-line altitudes. *Computers & Geosciences* 82: 55–62.
- Pellitero R, Rea BR, Spagnolo M et al. (2016) GlaRe, a GIS tool to reconstruct the 3D surface of palaeoglaciers. *Computers & Geosciences* 94: 77–85.
- Pfister C, Luterbacher J, Schwarz-Zanetti G et al. (1998) Winter air temperature variations in western Europe during the Early and High Middle Ages (AD 750–1300). *The Holocene* 8: 535–552.
- Prell WL and Kutzbach JE (1992) Sensitivity of the Indian monsoon to forcing parameters and implications for its evolution. *Nature* 360: 647–652.
- Raymo ME and Ruddiman WF (1992) Tectonic forcing of late Cenozoic climate. *Nature* 359: 117–124.
- Reimer PJ, Bard E, Baysliss A et al. (2013) IntCal13 and Marine13 radiocarbon age calibration curves 0–50,000 years cal BP. *Radiocarbon* 55: 1869–1887.
- Rood D, Burbank D and Finkel R (2011) Chronology of glaciations in the Sierra Nevada, California, from ^{10}Be surface exposure dating. *Quaternary Science Reviews* 30: 646–661.
- Seong Y, Owen LA, Bishop MP et al. (2007) Quaternary glacial history of the Central Karakoram. *Quaternary Science Reviews* 26: 3384–3405.
- Seong Y, Owen LA, Yi C et al. (2009) Quaternary glaciation of Muztag Ata and Kongur Shan: Evidence for glacier response to rapid climate changes throughout the Late Glacial and Holocene in westernmost Tibet. *Geological Society of America Bulletin* 121: 348–365.
- Smiraglia C (1997) Holocene variations of the Yanzigou Glacier (Gongga Shan Massif, DaXueshan, China). *Geografia Fisica e Dinamica Quaternaria* 20: 339–351.
- Steinhilber F, Abreu JA, Jürg B et al. (2012) 9,400 years of cosmic radiation and solar activity from ice cores and tree rings. *Proceedings of the National Academy of Sciences of the United States of America* 109: 5967–5971.
- Stone JO (2000) Air pressure and cosmogenic isotope production. *Journal of Geophysical Research: Solid Earth* 105: 23753–23759.
- Su Z and Shi Y (2002) Response of monsoonal temperate glaciers to global warming since the Little Ice Age. *Quaternary International* 97–98: 123–131.
- Thompson LG, Yao T, Davis ME et al. (2006) Holocene climate variability archived in the Puruogangri ice cap on the central Tibetan Plateau. *Annals of Glaciology* 43: 61–69.
- Wang J, Kassab C, Harbor JM et al. (2013) Cosmogenic nuclide constraints on late Quaternary glacial chronology on the Dalijia Shan, northeastern Tibetan plateau. *Quaternary Research* 79: 439–451.
- Wang Z (1991) The glacier and environment in the middle sector of Tianshan and the eastern sector of Qilianshan since the little ice age. *Acta Geographica Sinica* 46: 160–168 (in Chinese with English Abstract).
- Xu X and Yi C (2014) Little Ice Age on the Tibetan Plateau and its bordering mountains: Evidence from moraine chronologies. *Global and Planetary Change* 116: 41–53.
- Yao T, Shi Y and Thompson LG (1997) High resolution record of paleoclimate since the Little Ice Age from the Tibetan ice cores. *Quaternary International* 37: 19–23.
- Yao T, Thompson LG, Mosbrugger V et al. (2012a) Third Pole Environment (TPE). *Environmental Development* 3: 52–64.
- Yao T, Thompson LG, Yang W et al. (2012b) Different glacier status with atmospheric circulations in Tibetan Plateau and surroundings. *Nature Climate Change* 2: 663–667.
- Zhang Z (1988) The glacier variations on the northwestern slope in Namcha Barwa since the last glaciation. *Journal of Glaciology and Geocryology* 10: 180–188 (in Chinese with English Abstract).
- Zheng B and Ma Q (1994) The glacier variation, climatic change and the river valley development in the Holocene on the Gongga Mountains. *Acta Geographica Sinica* 49: 500–508.
- Zhu H, Xu P, Shao X et al. (2013) Little Ice Age glacier fluctuations reconstructed for the southeastern Tibetan Plateau using tree rings. *Quaternary International* 283: 134–138.
- Zhu L, Wu Y, Wang J et al. (2008) Environmental changes since 8.4 ka reflected in the lacustrine core sediments from Nam Co, central Tibetan Plateau, China. *The Holocene* 18: 831–839.